General Disclaimer

One or more of the Following Statements may affect this Document

- This document has been reproduced from the best copy furnished by the organizational source. It is being released in the interest of making available as much information as possible.

- This document may contain data, which exceeds the sheet parameters. It was furnished in this condition by the organizational source and is the best copy available.

- This document may contain tone-on-tone or color graphs, charts and/or pictures, which have been reproduced in black and white.

- This document is paginated as submitted by the original source.

- Portions of this document are not fully legible due to the historical nature of some of the material. However, it is the best reproduction available from the original submission.

A STUDY OF THE IMMUNITY OF FM DISCRIMINATORS TO 2π FREQUENCY IMPULSES

Frank F. Carden
Associate Professor

George L. Davis
Research Assistant

Lawrence R. Kelly
Research Assistant

William P. Osborne
Research Assistant

Communications Research Group
Electrical Engineering Department
New Mexico State University
Las Cruces, New Mexico

ABSTRACT

This paper reports the results of an investigation of the frequency impulse response of several FM discriminators. Experimental data are presented which display an impulse immunity of the phase-lock loop, as a result of rejection of a class of "fast" impulses. The results of a computer study for the phase-lock loop verify this. Experimental results for the pulse-averaging discriminator are also presented.

INTRODUCTION

The possibility of threshold extension in FM systems has created interest in the mechanism of this extension. The realization of threshold extension, using specific detectors and/or detector adjuncts, requires a knowledge of the low signal to noise behavior of these detectors. That behavior is the concern of this paper. Rice [1] has studied the threshold region for the ideal detector by considering the noise to be the super-position of "click" noise impulses and a gaussian noise component. The impulsive noise has a spectrum that is relatively flat across the bandwidth of the post-detection filter, and is proportional to the average number of click events per second. This impulsive noise may be reduced by a detector which rejects a fraction of the incoming impulses, or by a detector adjunct which senses the impulse and takes action to prevent its passage through the remainder of the system. The phase-lock loop operates in the first mode, rejecting a class of "fast" impulses.

The impulse event in FM systems is a random phenomenon, which may be depicted as in figures 1, 2, and 3. Figure 1 is a phasor diagram of an unmodulated carrier of amplitude Q and additive noise n(t). The noise phasor oscillates randomly about point Q. The impulse event occurs when the noise phasor assumes values such as to cause the resulting envelope, R, to make a complete cycle about the origin, causing θ to increment by 2π. Figure 2 displays the phase θ during the event, and figure 3 shows the frequency modulation produced. The weight of the impulse is approximately 2π. Rice [1] has investigated this noise term for the case of the ideal FM discriminator. Although this noise is not strictly impulsive, the approximation is valid for filter bandwidths much less than $1/\delta$, the event duration. The approximation of the event by a pulse is used in the experimental and theoretical work contained in this paper. If the filter bandwidths are small compared to $1/\delta$, the noise power in the output is proportional to the number of events per unit time [1]. Therefore, an FM discriminator which rejects some of the impulses will display an enhanced threshold characteristic over the ideal detector.

An ideal discriminator (whose output is θ) would pass all the impulses, and the filter output per event would approach the impulse response of the filter. Therefore, this detector offers no rejection capabilities.

The experimental results for the pulse averaging detector are shown in figures 4 through 6. The square pulse represents the input impulse, and is superposed on the response curve. Although the pulse amplitude in figure 6 is 50% greater than in figure 5, maintaining an area of 2π, the output has not changed significantly from figure 5 to figure 6. The output is approaching the impulse response of the filter used after the detector

which for this case is

$$h(t) = \alpha t e^{-\alpha t} \qquad t > 0 \qquad (1)$$

From these results, it is noted that the pulse-averaging detector is operating as an ideal detector, followed by a low-pass filter with an h(t) as in equation (1). All the input impulses are passed.

Results for the phase-lock loop are shown in figures 8 through 16. Figures 8 through 10 are experimental data, and 11 through 16 are computer solutions for the loop. Figures 14, 15, and 16 are phase error-time protraits corresponding to figures 11, 12, and 13, respectively. The computer data are hyperplane projections of the state space solutions of the set

$$\begin{bmatrix} \dot{Y}_1 \\ \dot{Y}_2 \end{bmatrix} = \begin{bmatrix} 0 & 1 \\ 0 & -2\,\xi\omega_n \cos Y_1 \end{bmatrix} \begin{bmatrix} Y_1 \\ Y_2 \end{bmatrix} + \begin{bmatrix} 0 \\ \omega_n^2 \sin Y_1 + \ddot{\Theta}_i(t) \end{bmatrix} \qquad (2)$$

where Y_1 is the phase error, Y_2 the frequency error, and $\Theta_i(t)$ the input phase.

The operation of the loop clearly shows its non-linear properties as the pulse amplitude becomes larger (compared to ωn). Figure 13 corresponds to the experimental results of figure 10 for the case of no significant output. The parameters of interest in describing when the rejection takes place are ωn, ξ (loop parameters), and $\Delta\omega$ (the input pulse amplitude). Figure 13 depicts the results when $(\Delta\omega/\omega n) = 12.5$, and $\xi = .3$. The pulse is rejected and the phase error increments by 2π, indicating that the loop has skipped a cycle in the process. Figures 14 and 15 indicate that, although phase lock has been broken, the loop has not skipped a cycle and the pulse was not rejected. For both of these cases $(\Delta\omega/\omega n) = 1.25$ and $\xi = .3$. Data presented in [2] indicate the location of the first separatrix for a second order phase-lock loop is

$$\frac{\Delta\omega_c}{\omega_n} \approx 2 + \sqrt{2}\,\xi$$

That is, for a step size (normalized) $\frac{\Delta\omega}{\omega_n} > 2 + \sqrt{2}\,\xi$, the loop will skip at least one cycle before relocking. Based on the data and this relationship, it appears that, if the input impulse has an amplitude greater than $5(\Delta\omega_c)$, the loop will reject the impulse and skip a cycle during the event.

SUMMARY

The phase-lock exhibits a click noise immunity not displayed by the ideal, or the pulse-averaging, FM discriminator to a class of "fast" impulses. The pulse-averaging detector passes the impulses as an ideal discriminator yielding an output determined by the post-detection filter. The phase-lock loop rejects (negligible response to) those impulses whose amplitude exceeds a multiple of its first separatrix location.

REFERENCES CITED

[1] Rice, S.O. "Noise in FM Receivers," Proc. Sym. on Time Series Analysis, M. Rosenblatt, Wiley, 1963.

[2] Carden, Lucky, Swinson. "The Quasi-Stationary and Transient Behavior of Non-Linear Phase-Lock Loops," SWIEEE, 1967 Record, Dallas.

This work was supported by NASA grant #NGR-32-003-037

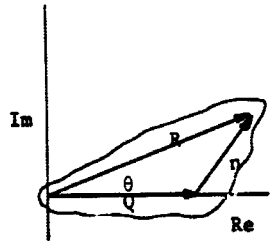

Figure 1. Impulse Event, Phasor Diagram

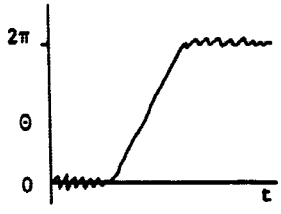

Figure 2. Impulse Event Phase vs Time

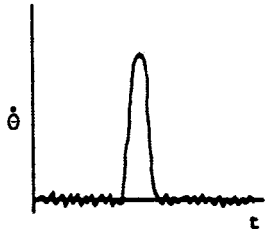

Figure 3. Impulse Event Frequency Impulse

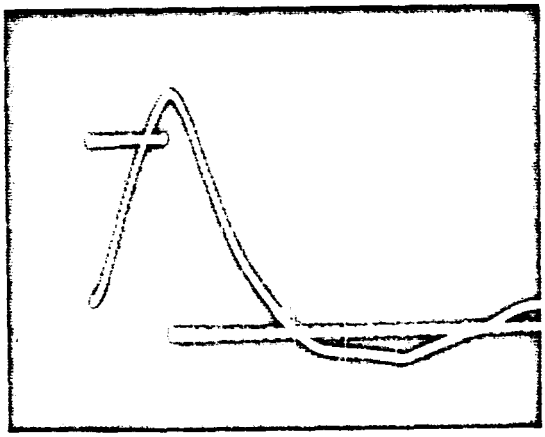

Figure 4. Demodulated Output, Pulse Averaging Detector. Experimental Results.

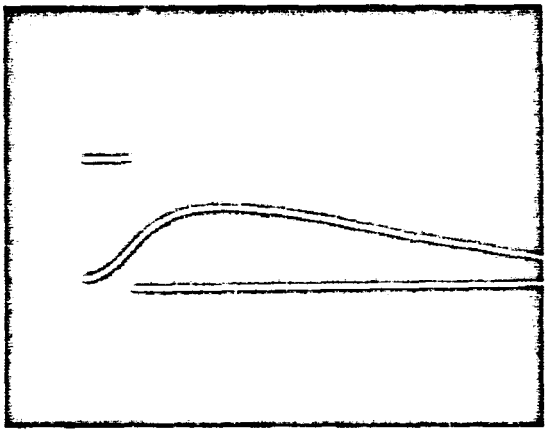

Figure 5. Demodulated Output, Pulse Averaging Detector. Experimental Results.

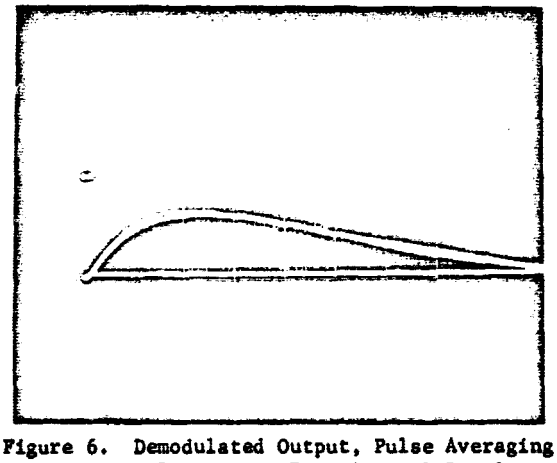

Figure 6. Demodulated Output, Pulse Averaging Detector. Experimental Results.

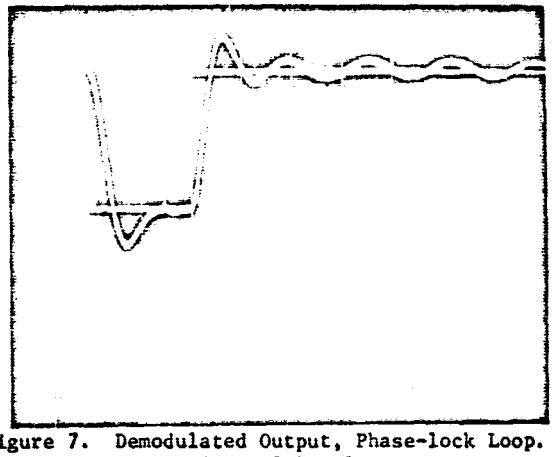

Figure 7. Demodulated Output, Phase-lock Loop. Experimental Results.

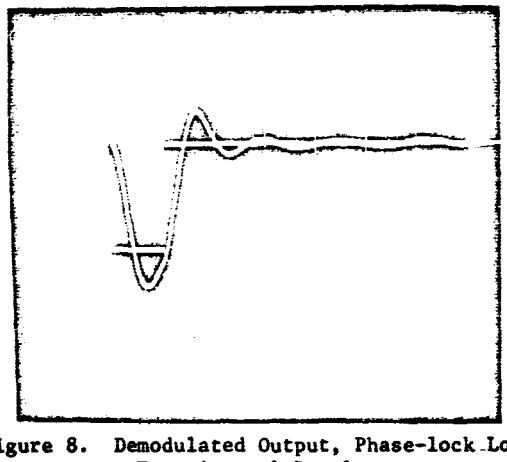

Figure 8. Demodulated Output, Phase-lock Loop. Experimental Results.

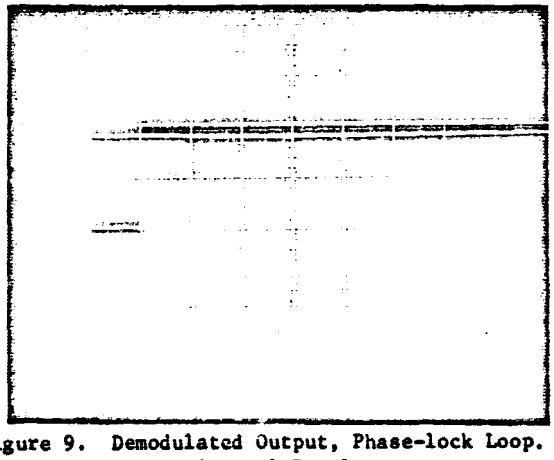

Figure 9. Demodulated Output, Phase-lock Loop. Experimental Results.

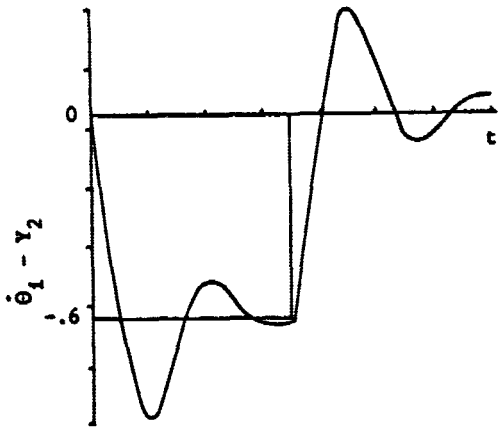

Figure 10. Demodulated Output, Phase-lock Loop. Computer Simulation.

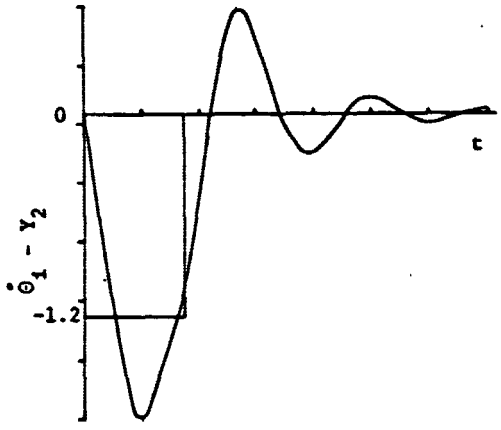

Figure 11. Demodulated Output, Phase-lock Loop. Computer Simulation.

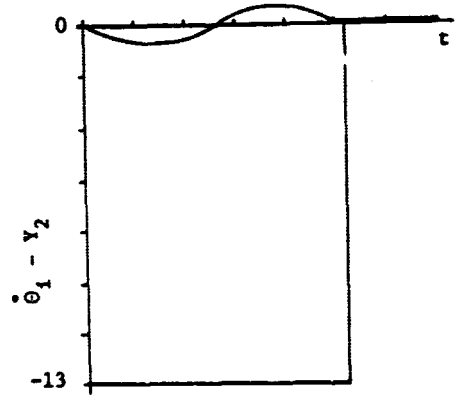

Figure 12. Demodulated Output, Phase-lock Loop. Computer Simulation.

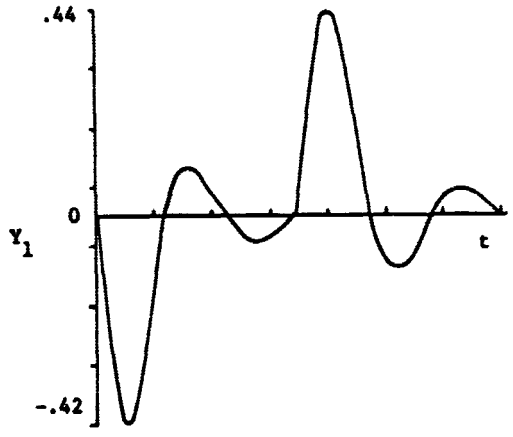

Figure 13. Phase Error vs Time, Phase-lock Loop. Computer Simulation.

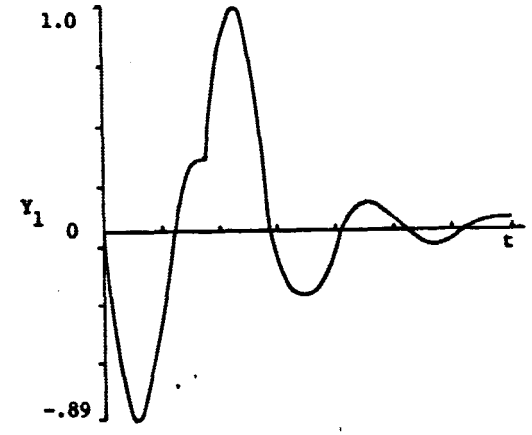

Figure 14. Phase Error vs Time, Phase-lock Loop. Computer Simulation.

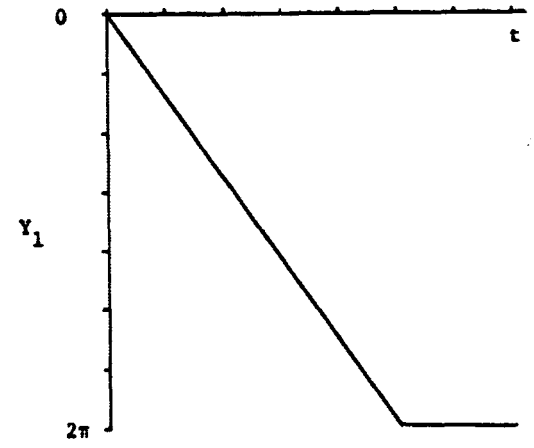

Figure 15. Phase Error vs Time, Phase-lock Loop. Computer Simulation.